

Original Article

# Synergistic degradation of catechin and minocycline hydrochloride in alkaline solution

Shiuh-Tsuen Huang<sup>a,b</sup>, Shwu-Yuan Lee<sup>c</sup>, Yuan-Jia Ju<sup>d</sup>, Ching-Chuan Chen<sup>d</sup>, Meei-Ju Yang<sup>e</sup>, Yu-Min Tzou<sup>b,\*</sup>, Ji-Yuan Liang<sup>d,\*</sup>

<sup>a</sup>Department of Science Education and Application, National Taichung University of Education, No. 140, Minsheng Rd., West District, Taichung City 403514, Taiwan

<sup>b</sup>Department of Soil and Environmental Sciences, National Chung Hsing University, No. 145 Xingda Rd., South District, Taichung City 402202, Taiwan

<sup>c</sup>Department of Tourism and Leisure, Hsing-Wu University, No.101, Sec.1, Fenliao Rd., Linkou District, New Taipei City 24452, Taiwan

<sup>d</sup>Department of Biotechnology, Ming-Chuan University, No. 5, Deming Rd., Guishan District, Taoyuan City 333, Taiwan

<sup>e</sup>Industry Service Section, Tea and Beverage Research Station, No.324 Chung-Hsing Rd., Yangmei District, Taoyuan City, 326011, Taiwan

## ARTICLE INFO

### Keywords:

Antibiotic  
Basification  
Catechin  
Minocycline  
Polyphenol

## ABSTRACT

Minocycline hydrochloride (MCH) is a broad-spectrum antibiotic commonly found in aquatic environments that can adversely affect aquatic ecosystems. Catechin, known for its low chemical stability, can undergo oxidative degradation under alkaline conditions. In this study, we used catechin basification to develop a method for degrading MCH and determined the effects of MCH degradation on bacterial growth. Approximately 38.0 and 65.4% of catechin was removed, with dimeric A- and B-type proanthocyanidins being formed, owing to the reduction of catechin via electron transfer after incubation at pH 10 for 2 and 24 h, respectively. MCH is stable in alkaline conditions but unstable when subjected to catechin in alkaline solutions. The percentages of degraded MCH and catechin were 57.1 and 65.4%, respectively, when mixed and incubated at pH 8 for 24 h. When MCH was incubated at pH 10 in the presence of catechin for 2 and 24 h, 62.3% and 87.4% of MCH and 56.2% and 98.3% of catechin were degraded, respectively, owing to the electron transfer induced by catechin basification, suggesting that the synergistic degradation of catechin and MCH is enhanced in alkaline solutions. The changes in the structure of MCH in the MCH-catechin system were confirmed by an ion signal at  $m/z$  472, namely, the molecular formula  $C_{23}H_{27}N_3O_8$ , and a mass of 473.5 g/mol. The effects of MCH and the degraded MCH on bacterial growth curves were examined. The treatment of MCH upon mixing with catechin, followed by 2h incubation at pH 8, led to bacterial growth rates of 0.037 and 0.057  $h^{-1}$ , respectively. After treatment with MCH-catechin, the bacterial growth curve steepened, indicating that MCH degradation reduces its antimicrobial activity under alkaline conditions. The results of this study highlight the potential for developing a simple and safe method to degrade MCH using catechin in alkaline conditions.

## 1. Introduction

Tetracyclines (TCs), a class of broad-spectrum antibiotics, inhibit protein synthesis in microorganisms by disrupting the binding of aminoacyl-transfer ribonucleic acid to the bacterial ribosome [1]. TCs are used to treat animal diseases and as sub-therapeutic growth promoters in various ways [2]. After systemic administration, >70% of TCs in animals or humans are excreted through feces and urine [3]. It is important to note that the unrestricted release of wastewater containing pharmaceuticals into natural water bodies or sewers leads to a different level of contamination [4,5]. Waste containing TCs poses a critical threat to the environment [6], and the removal of TCs from waste is crucial for the preservation of ecosystems.

Minocycline hydrochloride (MCH) is an antibiotic belonging to the TC class and is used to treat various infections [7]. MCH comprises a linearly fused tetracyclic structure (rings labelled A, B, C, and D) with a dimethylamino group at position 7 and, unlike some of its TC counterparts, no methyl or hydroxyl groups at position 5, as shown in

Figure 1(a). In solution, TCs become unstable when irradiated with UV light [8]. However, MCH is more stable under blue light irradiation (BLIA) than doxycycline hyclate (DCH). MCH is less photosensitive than DCH because of the dimethylamino group on ring D, which stabilizes MCH during photodegradation, whereas DCH lacks a similar amino group [9]. Waste containing MCH poses a serious environmental threat, necessitating its removal from wastewater. The photodegradation procedures are often used to degrade TCs. UV irradiation alone is less efficient for MCH removal. Metal-based catalysts, particularly those containing heavy metals such as ferric oxide [10], ferrous or ferric ions/hydrogen peroxide [11], nano-magnetite compounds [12], strontium titanate [13], titanium (IV) oxide [14,15], and zinc oxide [16,17] treated with visible or UV irradiation are often used to enhance the photocatalytic degradation of TCs, particularly in MCH. However, UV radiation and heavy metals are toxic. Furthermore, a green tea/ferrous ion system reductively degrades 1,1,1-trichloroethane under alkaline conditions (pH 10) by creating an electron-rich environment and initiating interactions between green tea and ferrous ion [18].

### \*Corresponding authors:

E-mail addresses: ymtzou@dragon.nchu.edu.tw (Y.-M. Tzou), jiyuanl@gmail.com (J.-Y. Liang)

Received: 16 December, 2024 Accepted: 27 April, 2025 Epub Ahead of Print: 25 July 2025 Published: 04 August 2025

DOI: 10.25259/AJC\_274\_2024

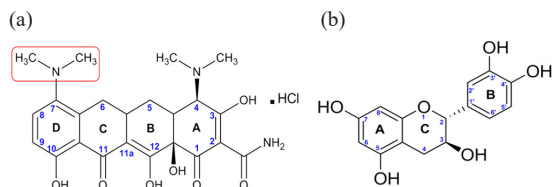


Figure 1. Chemical structures of (a) MCH and (b) catechin.

Nevertheless, polyphenols are naturally occurring organic compounds with phenolic hydroxyl groups [19]. Under alkaline conditions, the dissociation of a proton from the hydroxyl group of polyphenol forms a phenolate anion and creates an electron-rich environment. Polyphenols are potential alternatives to metal-based catalysts.

Catechin is a polyphenol abundant in chocolate, grapes, green tea, wine, and numerous other plant species. For example, polyphenols account for approximately 10%-30% of the dry weight of green tea leaves [20]. Among the polyphenols found in green tea, 80% are catechins, which exhibit anti-ageing, antioxidant, and antibacterial properties [21-23]. As shown in Figure 1(b), catechin is an organic compound belonging to the flavan class and is characterized by five hydroxyl groups attached to its core structure.

The total phenol content of a sample is typically expressed in terms of its catechin equivalent, which is a quantitative standard. The Folin-Ciocalteu (FC) assay is commonly used to measure total polyphenol content in biologically relevant samples. Under acidic conditions, a mixture of polyphenols and FC reagent (FCR) is stable; however, under alkaline conditions, the dissociation of a proton from the hydroxyl group forms a phenolate anion, which reduces FCR, leading to the reduction of the mixture. This reaction, unique to alkaline conditions, results in a colour change via an electron transfer mechanism [24].

Catechin is chemically unstable and readily oxidized in aqueous solutions [25]. Beverages containing catechins undergo oxidative and non-enzymatic browning reactions when significant pH changes occur [26]. Previous studies have shown that catechins in green tea are highly unstable in alkaline solutions (pH > 8) and can degrade completely within mins, whereas they exhibit greater stability in acidic solutions (pH < 4) [27]. In aqueous alkaline solutions, catechin loses its hydrogen atoms during oxidation and forms a semiquinone intermediate before further oxidation to form quinone [28,29]. Although stable under acidic conditions, catechin is significantly unstable when subjected to heat treatment at alkaline or neutral pH [30]. Chen *et al.* demonstrated that, under alkaline conditions, catechin undergoes esterification with dicarboxylic acids as the temperature increases [31]. Using high-performance liquid chromatography (HPLC) and mass spectrometry (MS), they also found that, under heat treatment at pH 8, catechin is degraded via the breaking of its ether linkage and oxidation to form an isomeric intermediate [30].

Catechin is also unstable under light irradiation at alkaline or neutral pH. Under weak alkaline conditions and BLIA, catechin generates B-type proanthocyanidins and oxidized quinone intermediates, with anionic superoxide radicals forming simultaneously in a photooxidation reaction [23-32]. This process inhibits the growth of *Acinetobacter baumannii* (*A. baumannii*) by at least 4 log units and deactivates the multi-drug-resistant strain of the bacterium.

*Escherichia coli* (*E. coli*), which is commonly found in the digestive systems of animals, is often used as an indicator of pathogenic contamination in potable water or food systems. High levels of *E. coli* can cause severe food poisoning in humans and are sometimes responsible for food recalls [33]. *E. coli* can survive outside the body, making it an effective indicator for detecting fecal contamination in environmental samples [34]. Therefore, if the antimicrobial effectiveness of MCH is reduced through degradation, an environmentally friendly approach to wastewater treatment can be adopted.

Phenolic compounds, such as catechin, are unstable under alkaline conditions and readily dissociate into protons to form short-lived intermediates and radicals. These unstable intermediates and radicals can participate in various oxidation reactions, altering the chemical structures of the compounds involved. Waste containing MCH poses a

serious threat to the environment. The oxidation of catechins may lead to the degradation of MCH, thereby reducing its antimicrobial activity and indicating an environmentally friendly wastewater treatment approach. This study aims to determine the effects of catechin basification on the degradation of MCH and the effect of degraded MCH on the reduction in antimicrobial activity under alkaline conditions. By harnessing the oxidative properties of catechin under alkaline conditions, a method for effectively degrading harmful antibiotics in wastewater can be developed. The effect of degraded antibiotics via catechin treatment on the viability of bacteria is used as an indicator to measure the efficiency of the technique.

## 2. Materials and Methods

### 2.1. Chemicals

(+)-Catechin ( $C_{15}H_{14}O_6$ ) was purchased from Toronto Research Chemicals Inc. (Toronto, ON). MCH ( $C_{23}H_{28}ClN_3O_7$ ) was purchased from Tokyo Chemical Industry Co. (Tokyo, Japan). Monopotassium phosphate ( $KH_2PO_4$ ), dipotassium phosphate ( $K_2HPO_4$ ), and FCR were purchased from Sigma-Aldrich (St. Louis, MO). A Milli-Q system was used to prepare ultra-pure water for the aqueous solutions.

### 2.2. Effect of pH on (+)-catechin and MCH solutions

The effect of pH on catechin and MCH was determined using an enzyme-linked immunosorbent assay (ELISA) reader provided by Thermo Fisher Scientific (Multiskan, Waltham, MA). Solutions were prepared as follows: (A) catechin (1 mM) was dissolved in 0.1 M phosphate-buffered saline (PBS) (pH 6, 8, and 10); (B) MCH (0.1 mM) was dissolved in PBS (pH 6, 8, and 10); and (C) a mixture of 0.1 mM MCH and 1 mM catechin was dissolved in PBS (pH 6, 8, and 10). Portions of the MCH and catechin solutions were incubated in the dark for 2 or 24 h. The absorbance of catechin solutions was recorded in the wavelength range of 300-800 nm using an ELISA reader.

### 2.3. Effect of pH on a mixture of catechin and MCH solution using a high-performance liquid chromatography-mass spectrometry (HPLC-MS)

The effect of pH on catechin and MCH solutions in PBS was evaluated using HPLC-MS, as described in previous studies [23-32]. Solutions were prepared as described in Section 2.2. The solutions were analysed using an Agilent 1200 Series HPLC system coupled with a 6410B triple quadrupole tandem MS equipped with electrospray ionization (ESI) as the ionizing source (Agilent Technologies, Palo Alto, CA). The MS analysis was conducted in negative ion mode. The operating parameters were as follows: drying gas ( $N_2$ ) at a temperature and flow rate of 350°C and 11 mL/min, respectively; a nebulizer gas pressure of 50 psi; a capillary voltage of 3700 V; and a temperature of 280°C. Data were collected over a full-scan range of 100-1,000 atomic mass units (amu). The data were processed using Agilent Mass Hunter Workstation software (version B.06.00).

The solutions were eluted at 40°C using a Poroshell 120 EC-C18 column (length = 150 mm, inner diameter = 4.6 mm, and particle size = 2.7  $\mu$ m) provided by Agilent Technologies (Palo Alto, CA). The solutions were prepared as described in Section 2.2 and filtered through a Millipore 0.45  $\mu$ m filter (Brighton, MA) before each analysis.

MCH and catechin, along with their degradation products, were separated using HPLC, with a mobile phase comprising methanol as solvent A and 0.1% formic acid as solvent B. The elution profile was established using a linear gradient of solvent A as follows: 0-3 min, 1%-10%; 3-10 min, 10%-20%; 10-16.5 min, 20%-75%; 16.5-20 min, 75%-50%; and 20-23 min, 50%-1%. For each analysis, a 5  $\mu$ L reaction solution was injected and eluted at a flow rate of 400  $\mu$ L/min.

### 2.4. Total phenol content

The total phenol content of catechin was evaluated using the FC method with slight modifications [31]. A phenolate anion produced by the dissociation of a phenolic proton can reduce FCR [24]. To perform the assay, we mixed 250  $\mu$ L of 1 mM catechin solution with 250  $\mu$ L

of 1 N FCR and 4.5 mL of PBS (pH 6, 8, and 10). The mixture was incubated at room temperature for 25 mins. The phenolic content was determined by measuring the extent of the reduction of  $\text{Mo}^{6+}$  to  $\text{Mo}^{5+}$ , with absorbance recorded at 730 nm [24] using an ELISA reader.

### 2.5. Effects of MCH and its degradation on bacterial growth curves

The *E. coli* DH5 $\alpha$  strain (NCBI Taxonomy ID: 668369) was obtained from the Bioresource Collection and Research Centre and cultured overnight in Lysogeny broth at 37°C. Following incubation, 1 mL of the culture was transferred into an Eppendorf micro-centrifuge tube and diluted to obtain an optical density of 0.2 at 600 nm ( $\text{OD}_{600}$ ) (approximately  $3.0 \times 10^6$  colony-forming units/mL). A 2.8 mL bacterial solution was then prepared, to which 0.2 mL of catechin (1 mM) and MCH (0.1 mM) or degraded MCH (D-MCH) was added. To prepare D-MCH, we dissolved 0.1 mM MCH and 1 mM catechin solutions in PBS at pH 8, followed by incubation for 2 h. The bacterial growth curves were monitored by measuring absorbance ( $\text{OD}_{600}$ ) using an ELISA reader. For each sample, measurements were obtained every 20 min for a 3 h incubation period at 37°C, with agitation at 150 revolutions per minute (rpm).

### 2.6. Statistics

All tests were conducted in triplicate. A one-way analysis of variance was used to determine the differences between the two samples. For comparisons between two groups with statistically significant differences, the unpaired Student's *t*-test was used. The results are presented as mean  $\pm$  standard deviation for each experiment, with statistical significance defined as  $p < 0.05$ .

## 3. Results and Discussion

### 3.1. Effect of pH on the color of catechin solution

The effect of pH on the colour of the catechin solution was assessed. As shown in Figure 2(a), the catechin in PBS (pH 6 and 8) was transparent; however, it turned yellow at pH 10. The absorption spectra of 0.17 mM catechin varied with pH. As shown in Figure 2(b), 0.17 mM catechin at pH 10 exhibited a peak at 426 nm.

### 3.2. HPLC-MS analysis of catechin at different pH values

Catechin and its oxidized products were analysed using HPLC-MS. The total ion chromatograms of catechin at different pH (6, 8, and 10) have been shown in Figure 3. Figure 3(a) shows the total ion chromatogram for catechin in PBS at pH 6, with a peak at 17.884 min corresponding to a mass-to-charge ratio ( $m/z$ ) of 289 (Figure 3e), indicating the presence of quasi-molecular anions  $[\text{M}-\text{H}]^-$ .

Following incubation at pH 10 for 2 h, the total ion chromatogram revealed the presence of several basification products eluted at 8.655, 11.549, 14.422, 15.631, 17.929, 18.458, and 19.190 mins, with ion fragments detected at  $m/z$  575, 575, 591, 577, 289, 303, and 289, respectively, as shown in Figure 3(c). After 24 h of incubation at pH 10, catechin decomposition was observed (Figure 3d). The basification products were eluted at 8.49, 11.4, 14.213, 14.758, 15.355, 16.213, 17.824, 18.399, and 19.190 mins, with ion fragments at  $m/z$  575, 575, 591, 577, 577, 287, 289, 303, and 289, respectively. The relative amount of 1 mM catechin after incubation was 100% at pH 6, 101.3%

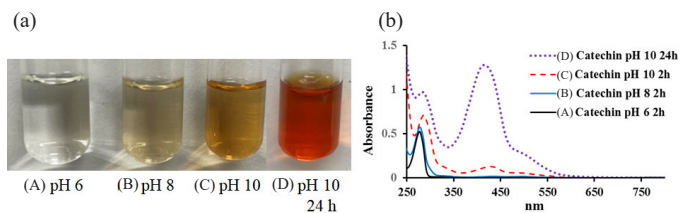


**Figure 2.** Changes in the (a) colour of 1 mM catechin and (b) absorption spectra of 0.17 mM catechin incubated at different pH levels: (A) 6, (B) 8, and (C) 10 for 2 h, and (D) 10 for 24 h.

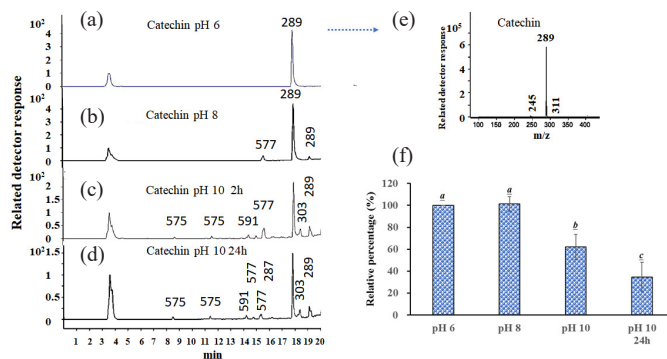


**Figure 3.** Total ion chromatograms of 1 mM catechin incubated at pH (a) 6, (b) 8, and (c) 10 for 2 h and (d) 10 for 24 h in the dark, as determined using HPLC-MS. The inset shows the mass spectrum of (e) catechin alone. (f) Relative content of 1 mM catechin incubated at pH 6, 8, and 10 for 2 h and at pH 10 for 24 h in the dark, as determined by HPLC-MS. Statistically significant differences ( $p < 0.05$ ) between the two groups are indicated by different letters above each bar.

at pH 8, and 62.0% at pH 10 after 2 h, and 34.6% at pH 10 after 24 h (Figure 3f).

### 3.3. Effect of pH on MCH

In Figure 4, the effect of pH on the colour of the MCH solution was also investigated. The MCH in PBS (pH 6, 8, and 10) was transparent, as shown in Figure 4(a). The absorption spectra of 0.1 mM MCH at different pH values are shown in Figure 4(b). At pH 10, a peak at 382 nm was observed for MCH.

### 3.4. HPLC-MS analysis of MCH at different pH values

The total ion chromatograms for MCH incubated at pH 6, 8, and 10 for 2 h and 10 for 24 h were acquired via HPLC-MS analysis and are shown in Figure 5. As shown in Figure 5(a), the total ion chromatogram of an aqueous MCH solution at pH 6 shows a peak at 18.8 min, corresponding to its elution, as confirmed by its molecular ion at  $m/z$  456 (Figure 5e). The intensity of the MS peak was obtained in  $[\text{M}-\text{H}]^-$  mode.

The MCH content after incubation at pH 6, 8, and 10 for 2 h and 10 for 24 h was determined using HPLC-MS. No statistically significant difference was observed between the relative percentages of MCH incubated at pH 8 and 10 for 2 h or at pH 10 for 24 h (Figure 5f).

As shown in Figure 4(b), the spectra of 0.1 mM MCH exhibited a red shift in the stimulated emission as the pH increased, indicating the behaviour of MCH under alkaline conditions. Notably, an isosbestic point was observed (Figure 4b), indicating the deprotonation of MCH. Proton and charge transfer studies have shown that MCH exists as  $\text{MCH}_2^+$  (neutral zwitterionic species),  $\text{MCH}^+$ , and  $\text{MC}^{2+}$  at pH 6.4, 9.0, and 11.3, respectively, with deprotonation occurring under alkaline conditions [35]. The relative percentage of MCH was consistent at pH 6, 8, and 10 after 2 h of incubation (Figure 5f). MS ionizes molecules to form molecular ions, providing information about their molecular weight, elemental composition, and fragmentation patterns. As shown

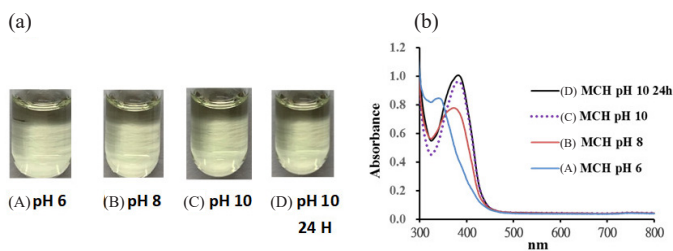


**Figure 4.** (a) Change in the colour of a 0.1 mM MCH solution incubated at pH (A) 6, (B) 8, and (C) 10 for 2 h and (D) 10 for 24 h. (b) Absorption spectra of a 0.1 mM MCH solution incubated at pH (A) 6, (B) 8, and (C) 10 for 2 h and (D) 10 for 24 h.

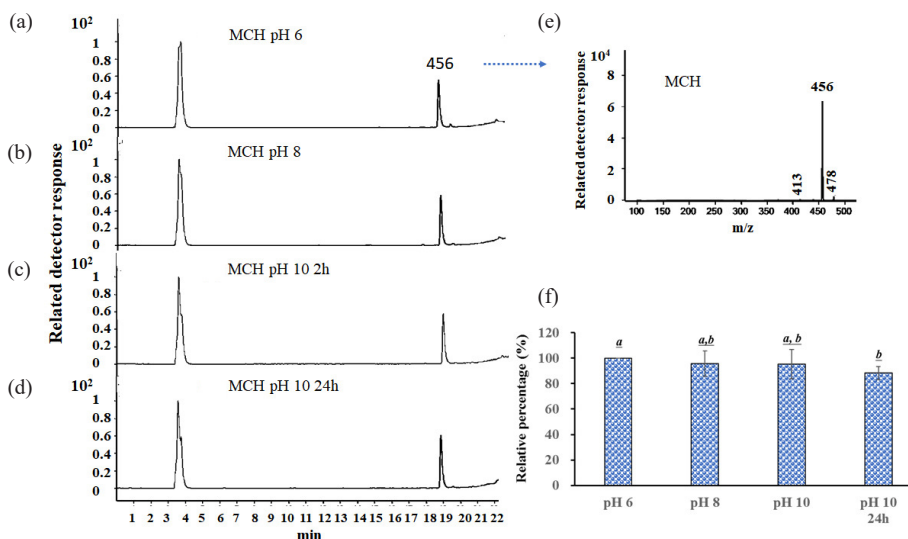


**Figure 5.** (a) Total ion chromatograms of a 0.1 mM MCH solution incubated at pH (a) 6, (b) 8, and (c) 10 for 2 h and (d) 10 for 24 h in the dark, as determined via HPLC-MS analysis. The inset shows the mass spectrum of (e) MCH alone. (f) Relative content of a 0.1 mM MCH solution after incubation at pH 6, 8, and 10 for 2 h and 10 for 24 h in the dark, as determined by HPLC-MS analysis. Statistical differences ( $p < 0.05$ ) between the two groups are indicated by distinct letters above each bar.

in Figure 5, the mass spectra of MCH at different pH values were consistent with that of deprotonated MCH, with a molecular weight of 456 Da, as determined by ESI.

### 3.5. Changes in catechin solution after the addition of MCH at pH 10

The effect of pH on catechin, as indicated by the observed colour change after the addition of MCH, was assessed. When 1 mM catechin was mixed with 0.1 mM MCH in PBS at pH 10 and incubated for 2 or 24 h, the solution turned yellow, as shown in Figure 6(a).

The spectra of a 1 mM aqueous catechin solution before and after the addition of a 0.1 mM MCH at pH 10 are shown in Figure 6(b). Upon the addition of MCH and subsequent incubation for 2 and 24 h at pH 10, peaks characteristic of catechin appeared at 412 and 431 nm, respectively (Figure 6b).

### 3.6. HPLC-MS analysis of catechin solution following the addition of an aqueous alkaline MCH solution

The MCH concentrations at pH 8 and 10 after incubation for 2 and 24 h were determined using HPLC-MS. The MCH concentrations after incubation at pH 6, 8, and 10 for 2 h and at pH 10 for 24 h showed no statistically significant differences, as shown in Figure 5(f). At pH 8, the concentrations of MCH (initial concentration = 0.1 mM) were 0.047 and 0.043 mM, corresponding to 47.3% and 42.9%, after 2 and 24 h of incubation with catechin, respectively, as shown in Figure 7(a). No statistically significant difference ( $p = 0.12$ ) was observed between the relative percentages of MCH at pH 8 for 2 and 24 h incubation

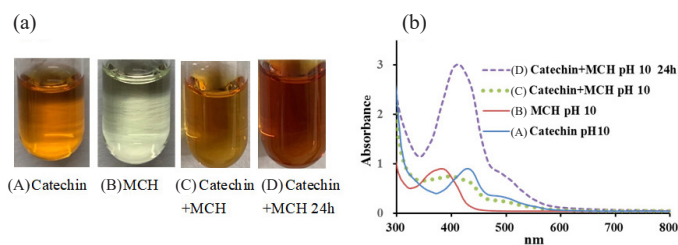


**Figure 6.** (a) Colour change of (A) 1 mM catechin, (B) 0.1 mM MCH, and (C) 0.1 mM MCH in the presence of 1 mM catechin and incubated for 2 h at pH 10, and (D) 0.1 mM MCH in the presence of 1 mM catechin and incubated for 24 h at pH 10. (b) Absorption spectra of (A) 1 mM catechin, (B) 0.1 mM MCH, and (C) 0.1 mM MCH in the presence of 1 mM catechin and incubated for 2 h at pH 10, and (D) 0.1 mM MCH in the presence of 1 mM catechin and incubated for 24 h at pH 10.

with catechin (Figure 7a). At pH 10, the concentrations of MCH were 0.038 and 0.013 mM, corresponding to 37.7% and 12.6%, after 2 and 24 h of incubation with catechin, respectively, as shown in Figure 7(a). These results indicate that the degradation of MCH is enhanced in the presence of catechin under alkaline conditions.

The catechin concentrations were determined at pH 8 and 10 after incubation for 2 and 24 h. No statistically significant difference ( $p = 0.28$ ) was observed between the relative percentages of catechin at pH 8 for 2 and 24 h incubation with MCH (Figure 7b). At pH 10, the concentrations of 1 mM catechin in the presence of 0.1 mM MCH were 0.438 and 0.017 mM after 2 and 24 h of incubation, respectively. The relative percentages of catechins were 62.0% and 34.6% after incubating catechin alone for 2 and 24 h at pH 10, respectively, as shown in Figure 3(f). As shown in Figure 7(b), the relative percentages of catechins in the presence of 0.1 mM MCH were 43.8% and 1.7% after 2 and 24 h of incubation at pH 10, respectively. These results indicate that catechin degradation is enhanced to some degree in the presence of MCH under alkaline conditions.

The total ion chromatograms obtained from the HPLC-MS analysis of catechins in the presence of MCH at pH 10 after incubation for 2 and 24 h have been shown in Figure 8. As shown in Figure 8(a), the total ion chromatogram of the MCH solution at pH 10 shows a peak at 18.8 min with fragmented ion species at  $m/z$  456. As shown in Figure 8(c), the total ion chromatogram of MCH was significantly reduced after 2 h of incubation with catechin at pH 10, with the basification products eluting at 14.743, 15.295, 17.802, 18.384, 18.884, and 19.107 min and characteristic ion fragments detected at  $m/z$  577, 577, 289, 303, 456, and 289, respectively. Figure 8(d) shows the further degradation of the total ion chromatogram of MCH after 24 h of incubation with catechin at pH 10, with the basification products (after adding MCH) eluting at 8.468, 11.341, 14.191, 14.601, 16.108, 17.794, 18.175, 18.369, 18.869, and 19.234 min and characteristic ion fragments detected at  $m/z$  575, 575, 591, 472, 287, 289, 287, 303, 456, and 303, respectively.

### 3.7. Total phenol content at different pH values

The effect of pH on the phenol content of catechin was evaluated using a modified FC method. As shown in Figure 9, the phenol content of catechin at pH 10 was approximately 1.64-fold higher than that at pH 6. According to the FC method for polyphenol analysis in aqueous alkaline solutions, phenolic compounds tend to dissociate into an anionic phenolate, which reduces  $\text{Mo}^{6+}$  in the FCR to  $\text{Mo}^{5+}$  via electron transfer [31]. However, catechin is unstable at pH 10 and undergoes significant decomposition via electron transfer.

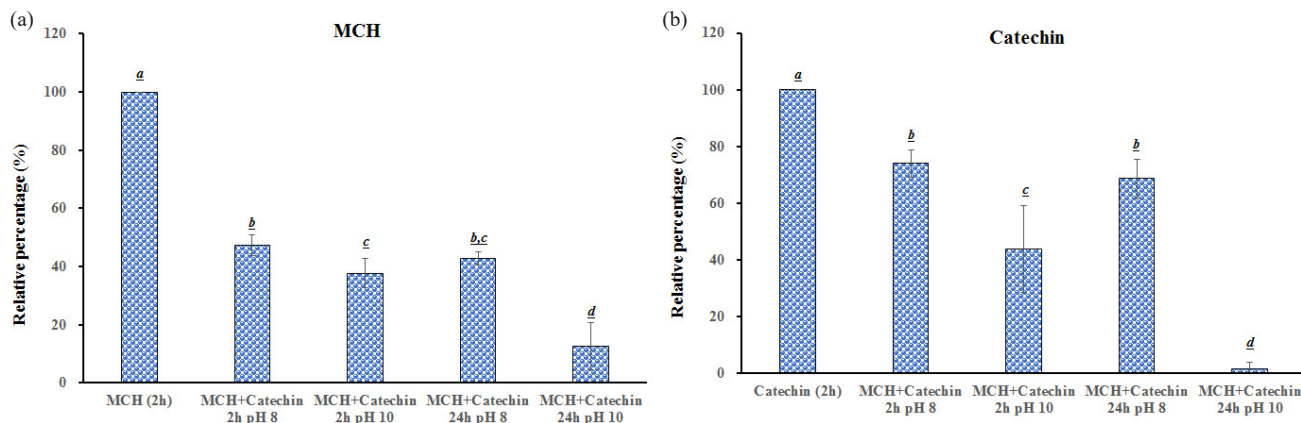


**Figure 7.** (a). Relative percentage of 0.1 mM MCH in the presence of 1 mM catechin after incubation for 2 and 24 h at pH 8 and 10. (b) Relative percentage of 1 mM catechin in the presence of 0.1 mM MCH after incubation for 2 and 24 h at pH 8 and 10, as determined by HPLC-MS analysis. Statistical differences ( $p < 0.05$ ) between the two groups are indicated by distinct letters above each bar.

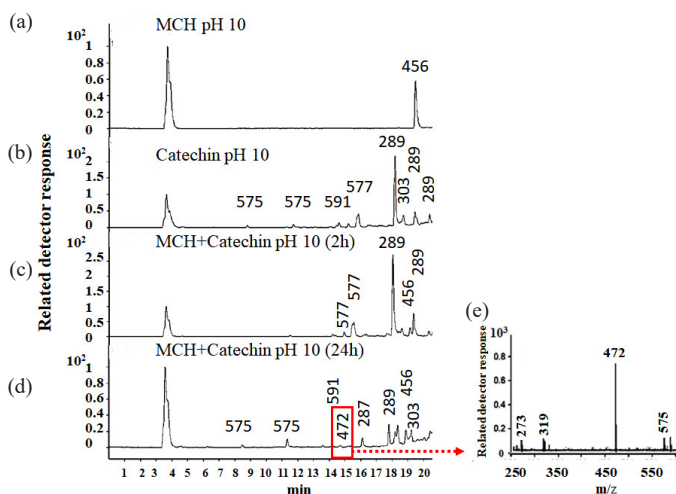


**Figure 8.** Total ion chromatograms obtained from HPLC-MS analysis at pH 10 for (a) 0.1 mM MCH incubated for 2 h, (b) 1 mM catechin incubated for 2 h, (c) 0.1 mM MCH in the presence of 1 mM catechin and incubated for 2 h, and (d) 0.1 mM MCH in the presence of 1 mM catechin and incubated for 24 h. The inset shows the mass spectrum of (e) degraded MCH (D-MCH) after basification in the MCH-catechin system.

### 3.8. Effects of incubating MCH in the presence of catechin on bacterial growth curves

MCH is a TC antibiotic that poses a significant environmental threat when TC-containing waste is released [6]. The effects of MCH and D-MCH on bacterial growth curves were examined. The bacterial growth curves for MCH and D-MCH over 0-3 h are shown in Figure 10. There was a significant difference ( $p < 0.05$ ) between the growth rate of D-MCH and MCH (Figure 10). The growth rate constants for D-MCH and MCH were 0.057 and 0.037  $\text{h}^{-1}$ , respectively, indicating that the MCH-catechin system reduces the antibacterial activity of MCH. Furthermore, D-MCH obtained via the MCH-catechin interaction exhibited lower antibacterial activity against *E. coli*, as shown in Figure 10.

Catechin is stable under acidic conditions; however, it is significantly unstable under neutral or alkaline conditions. The catechin spectra varied significantly for different pH values. As shown in Figure 2(b), the spectra of the catechin solution at pH 10 showed an absorbance band in the 350-450 nm range. This band can be attributed to the formation of chromogenic catechin derivatives induced by structural rearrangement in aqueous alkaline solutions. This study demonstrated that MCH degradation was significantly increased by the structural rearrangement of catechin incubated at pH 10.

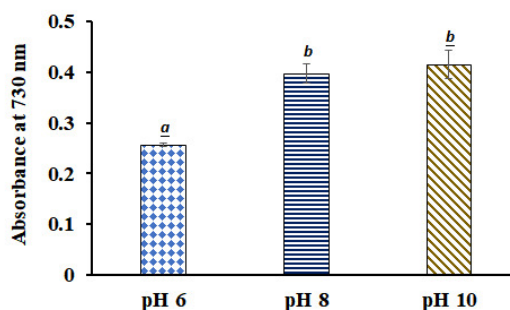


**Figure 9.** Effects of pH on 1 mM catechin in the Folin-Ciocalteu (FC) assay at pH 6, 8, and 10. Statistical differences ( $p < 0.05$ ) between the two groups are indicated by distinct letters above each bar.

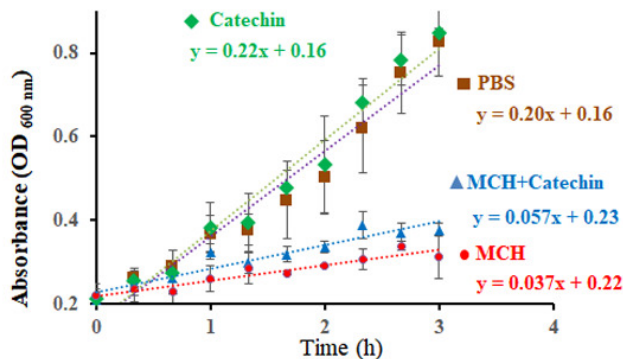


**Figure 10.** Effects of catechin, D-MCH, and MCH on *E. coli* growth curves at pH 8

The effect of catechin basification on MCH degradation was examined after incubation at pH 10. When incubated in the presence of 1 mM catechin at pH 10 in the dark for 24 h, 87.4% of MCH was degraded. The structural modification of MCH may significantly alter its properties. To maintain the antibacterial efficacy of TCs, each of the four linearly fused carbon-based rings must be six-membered [1]. Our previous study showed that TC degradation via riboflavin-5'-phosphate (FMN) photolysis markedly reduced the antimicrobial efficacy of TCs, leading to the formation of degraded TCs with the molecular formula  $\text{C}_{21}\text{H}_{22}\text{N}_2\text{O}_8$  [3]. The main ion fragment of MCH was detected at  $m/z$  456. However, after 2 h of incubation in the presence of catechin at pH 8 and 10, 52.7% and 62.3% of the MCH degraded, respectively. In addition, although the major ion fragment of MCH was detected

at  $m/z$  456, an ion fragment at  $m/z$  472 was observed for the MCH-catechin system at pH 10 (Figure 8). ROS-mediated TC degradation via FMN photolysis significantly decreases antimicrobial activity [3]. *E. coli* growth curves for MCH and D-MCH over 0-3 h are shown in Figure 10, with a growth rate of  $0.057 \text{ h}^{-1}$  for D-MCH and  $0.037 \text{ h}^{-1}$  for MCH. It shows that the D-MCH obtained from MCH-catechin treatment is efficient in the preservation of ecosystems due to its lower antibacterial activity. However, the limitations of this study are that (1) the degradation of MCH is reliant on the basification of catechin; i.e., the pH needs to be adjusted in aquatic systems, and (2) the *E. coli* (a Gram-negative bacillus) growth assay was inhibited in this study, so the effects of MCH-catechin upon basification on the growth of Gram-positive bacteria or protozoan parasites can be further studied by this system.

In solutions, TCs become unstable when irradiated with UV light [8]. However, MCH is more stable under BLIA than DCH. MCH is less photosensitive than DCH [9]. In addition, TC degradation by FMN under BLIA was significantly reduced due to the generation of reactive oxygen species (ROS) [3]. Previous studies have shown that catechin generates ROS during photolytic reactions under BLIA [36], which inhibits the growth of *A. baumannii* [23]. In this study, MCH was degraded by 69.9% after incubation at pH 10 for 2 h in the presence of 1 mM catechin under BLIA at  $6.0 \text{ mW/cm}^2$  (data not shown), compared with a 62.3% reduction under identical conditions without light treatment (Figure 7), whereas the photolysis of catechin under BLIA at  $6.0 \text{ mW/cm}^2$  for 2 h increased the degradation by 7.6%. It would be of interest to examine whether catechin-treated MCH, after exposure to visible light, could increase the degradation of MCH via ROS generated through a charge transfer process using catechin photolysis for future research.

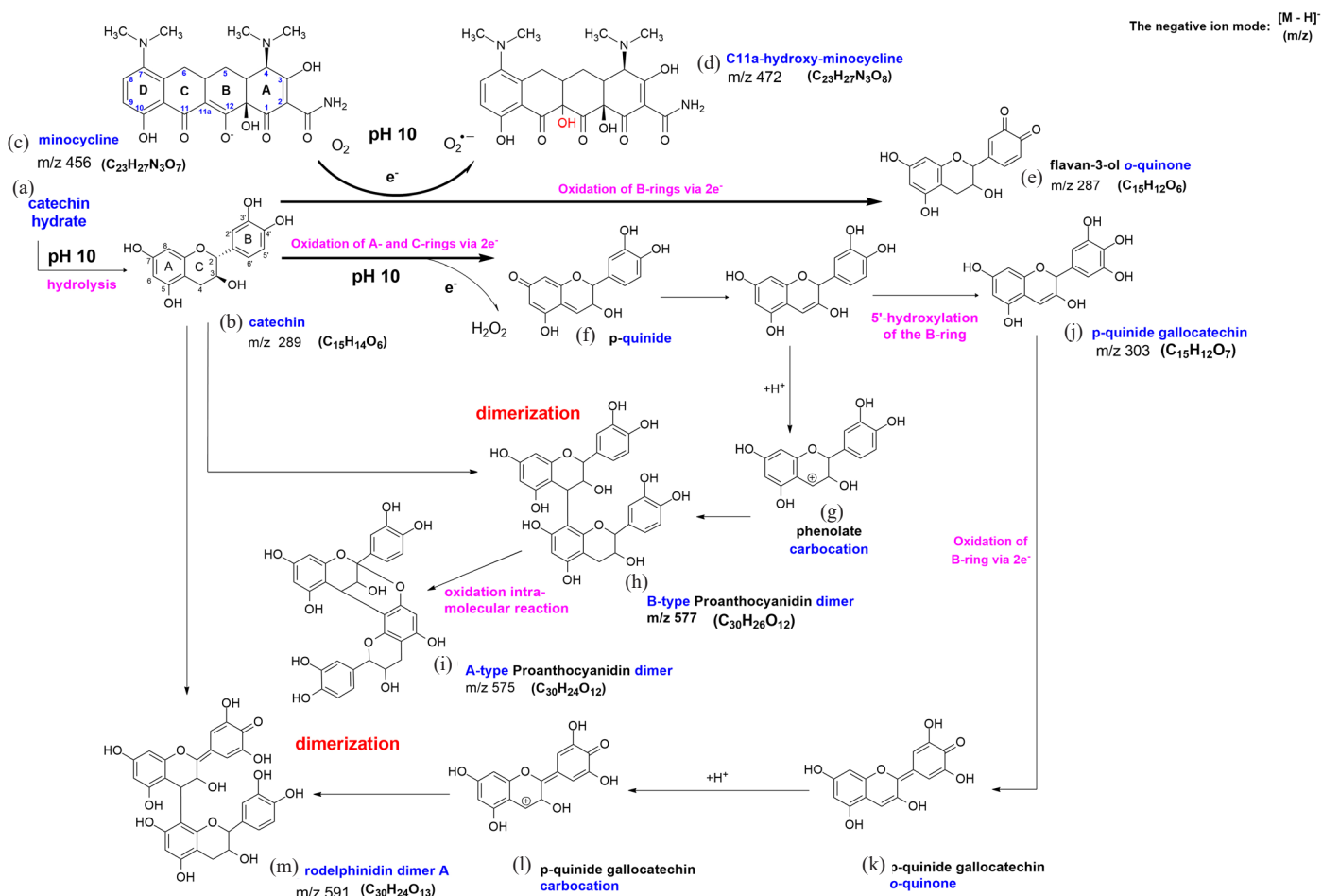


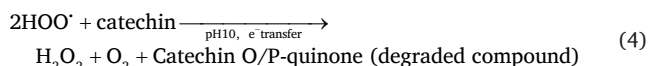
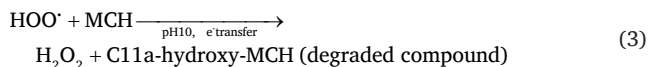
**Figure 11.** (a-m) Synergistic degradation mechanism of catechin and MCH in an alkaline solution. The strong alkaline conditions lead to increased hydrolysis and oxidation of both catechin and MCH. The products of catechin and MCH oxidation by atmospheric oxygen and base-catalysed reactions are analyzed by an HPLC-MS assay.

flavanols primarily arises from the *o*-hydroxyl groups on aromatic rings, which are directly related to ROS formation during flavanol autoxidation [37,41,42]. During catechin oxidation, anionic superoxide radicals and semiquinone intermediates play a significant role in the reaction because their stability increases with increasing pH, explaining the pH-dependent nature of the oxidation process [29]. The reaction mechanism of anionic superoxide radicals with phenolic derivatives involves a two-electron transfer process coupled with proton transfer in the transition state, as indicated by negative activation entropy values, which suggests solvent reorganization to facilitate proton transfer [43].

In this study, a mechanism is proposed for the formation of H<sub>2</sub>O<sub>2</sub> during the base-catalyzed oxidation of the interaction between MCH and catechin. The process involves reactions Eqs. (1)-(4), including the pH-dependent initiation of superoxide formation, and the redox reaction that involves MCH and catechin. In the final reaction, the redox reaction is driven by the hydroperoxyl radical, resulting in the formation of MCH and catechin redox reaction products and H<sub>2</sub>O<sub>2</sub>, and promotes the hydroxylation reaction.



then



MCH binds in a large, tunnel-shaped active site in close contact with catechin, a cofactor acting as a reductant, and forms pre-orientated adducts for regioselective hydroxylation to form C-11a-hydroxy-minocycline under aerobic conditions [44]. The C11a-C12 double bond of MCH was much more susceptible for free radicals to attack through an electron-withdrawing substituent from adjacent electron-donating groups of catechin, making C11a-C12 the most susceptible position for hydration [45] to hydroxylate by oxygen transfer from H<sub>2</sub>O<sub>2</sub> onto the aromatic ring, after which an intermediate epoxide is formed that can spontaneously rearrange into a hydroxyl group on C11a [46]. During this reaction, an intermediate  $\alpha$ -hydroxy ketone of MCH is produced. The enol tautomer of the  $\beta$ -diketone is an activated double bond in

which the keto-enol motif at C-11a/C-12 undergoes deprotonation, leading to the hydroxylation of C-11a and forming an  $\alpha$ -hydroxy ketone at the C-11a-C-12 position [47]. The product of the interaction between MCH and catechin at pH 10 has the molecular formula C<sub>23</sub>H<sub>27</sub>N<sub>3</sub>O<sub>8</sub> (*m/z* 472) from C<sub>23</sub>H<sub>27</sub>N<sub>3</sub>O<sub>7</sub> (*m/z* 456) of MCH, as shown in Figure 11(d) and Figure 12.

Flavanol (catechin) degradation occurs spontaneously via autoxidation, and the rate of autoxidation is significantly influenced by factors such as temperature, humidity, and pH. Owing to the stabilizing effects of intramolecular hydrogen bonding and the low-energy transformation of unsaturated conjugated systems, *o*-/*p*-polyhydroxy-substituted aromatic groups, such as catechol, pyrogallol, and quinol moieties, donate electrons more efficiently than their *m*-substituted counterparts, leading to the formation of the *o*-quinone derivatives found in the original sample [37-48].

The base-catalyzed oxidation of catechin involves three key steps: oligomerization, rearrangement, and hydroxylation [46]. The main oligomerization and rearrangement products formed by the oxidation of polyphenol and hydroxylation are structurally represented by oxygen transfer from H<sub>2</sub>O<sub>2</sub> onto the aromatic ring [46]. The roles of electron transfer and oxidative pathways in catechin degradation are as follows: the oxidation of B-rings via the 2e<sup>-</sup> pathway (PathI), and the oxidation path of A- and C-rings via the 2e<sup>-</sup> pathway (PathII), respectively.

Path I: Oxidation of catechin proceeds in two successive steps, with the final product being the *o*-quinone derivative flavan-3-ol *o*-quinone, as evidenced by the molecular ion peak at *m/z* 287 (C<sub>15</sub>H<sub>12</sub>O<sub>6</sub>), as shown in Figure 11(e).

Path II: Li and Deinzer highlighted that, for the accurate identification and characterization of proanthocyanidins, the following aspects need to be considered: 1. Molecular ion peaks (M-H) in the negative ion mode of MS, such as *m/z* 577 for B-type proanthocyanidin and *m/z* 575 and 591 for A-type proanthocyanidins derived from catechin monomeric units, indicate oligomer formation. 2. The fragmentation pathway described by Gu *et al.* provides insights into the hydroxylation of B-rings and bonding between monomeric units. In addition, quinone methide fragmentation, which defines the two monomeric units and the loss of H<sub>2</sub>O from the C-ring, indicates the presence of an epicatechin unit [49,50].

Herein, two types of oligomerizations were identified: proanthocyanidin dimers at *m/z* 577 and prodelfinidin dimers at *m/z* 591. Mechanistically, proanthocyanidins are formed via the two-electron oxidation of the A-ring of catechin, yielding a *p*-quinone intermediate, as shown in Figure 11(f). Alternatively, the formation of a carbocation at C-4 of catechin can be hypothesized, which would occur via two-electron oxidation followed by loss of a proton, producing a phenolate carbocation, as shown in Figure 11(g). The phenolate carbocation acts

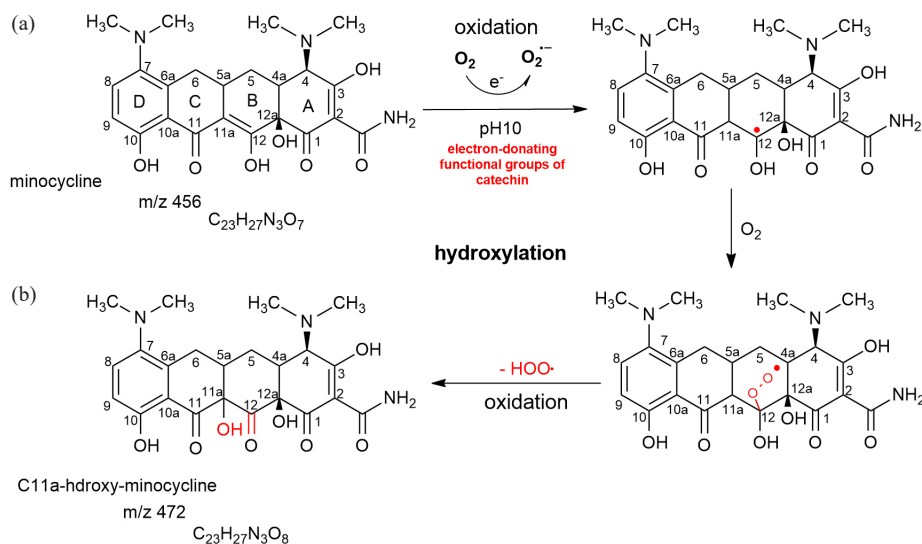


Figure 12. Hydroxylation of minocycline (a) minocycline and (b) C-11a-hydroxy-minocycline.

as a strong electrophile and can be attacked by catechin molecules, leading to the formation of catechin dimeric oxidation products, particularly the B-type proanthocyanidin dimer at  $m/z$  577 ( $C_{30}H_{26}O_{12}$ ) [51,52] (Figure 11h). Furthermore, the B-type proanthocyanidin dimer converts into an A-type dimer through intramolecular oxidation, which shows a molecular ion peak at  $m/z$  575 [52,53], as shown in Figure 11(i). The second type, the prodelphinidin dimer at  $m/z$  591, indicates the presence of an A-type dimer formed from gallo catechin quinide and catechin, as shown in Figure 11(m). During the initial stage of dimer formation, the two-electron oxidation of the A- and C-rings produces a *p*-quinide intermediate with a rearranged structure.

The ions at  $m/z$  303, identified as *p*-quinone gallo catechin, were formed via a series of processes involving the hydrolysis, oxidation, and 5'-hydroxylation of the B-ring. Flavan-3-ols are non-planar owing to their saturated C-3 element and represent the most structurally complex subclass of flavonoids, which can form gallo catechin via hydroxylation at the C-5' position of the B-ring [54,55]. These derivatives are short-lived intermediates and undergo polymerization in aqueous solutions at high pH [37], as shown in Figure 11(j). Subsequently, a *p*-quinone gallo catechin carbocation can also form after the two-electron oxidation of the B-ring, and a structural rearrangement process promotes prodelphinidin dimer A generation, as evidenced by an ion peak at  $m/z$  591 (Figures 11(k), (l), and (m), respectively).

Under BLIA, catechin undergoes photolysis and polymerization, as indicated by the characteristic  $m/z$  ion signal at 577, corresponding to B-type proanthocyanidin [38]. This study demonstrated that, under alkaline conditions (pH 10), both A- and B-type proanthocyanidins were generated and identified by their characteristic ion fragments at  $m/z$  577 and 575, respectively, owing to condensation reactions. The catechin dimer is present in many foods, including apples, blueberries, chocolate, and cranberries [56-58]. In addition to their role as cancer chemopreventive and anti-inflammatory agents, proanthocyanidins can also alleviate the risk of cardiovascular mortality [59]. Therefore, the strengths of this study are as follows: (1) the basification of flavan-3-ols under alkaline conditions effectively produces proanthocyanidin, a naturally occurring antioxidant; (2) catechin is a natural compound with no toxicity in aquatic systems, and as such, the basification of catechin provides a safe means of MCH degradation in water; (3) catechin, when mixed with MCH in an alkaline solution, significantly enhances MCH degradation, indicating potential environmental applications; and (4) the degraded MCH obtained from MCH-catechin treatment is efficient in the preservation of ecosystems due to its lower antibacterial activity.

#### 4. Conclusions

Phenolic compounds are unstable and readily dissociate phenolic protons to generate phenolate anions in alkaline solutions. The reduction of catechin was enhanced in this study, leading to the formation of dimeric proanthocyanidin via electron transfer at high pH. The synergistic degradation of catechin and MCH occurred in alkaline solutions. Catechin basification can support an electron donor process for the degradation of MCH. Under alkaline conditions, the structure of MCH is altered by a base-induced electron transfer process caused by the oxidation of catechin. D-MCH obtained from MCH-catechin treatment was confirmed by an ion signal at  $m/z$  472 and exhibited lower antibacterial activity against *E. coli*. These structural changes indicate the formation of less toxic or less bioactive compounds, suggesting that the basification of catechin can effectively minimize the harmful effects of MCH in aquatic environments. Therefore, catechin basification is an easy and safe method for degrading MCH in solution, providing a promising means of suppressing antibiotic pollution in aquatic ecosystems and reducing the harmful effects on microbial communities.

#### CRedit authorship contribution statement

**Shiuh-Tsuen Huang:** Data curation, Methodology, Writing-original draft. **Shwu-Yuan Lee:** Project administration. **Yuan-Jia Ju:** Formal analysis. **Ching-Chuan Chen:** Formal analysis. **Meei-Ju Yang:**

**Resources.** **Yu-Min Tzou:** Validation, Writing-review & editing. **Ji-Yuan Liang:** Investigation, Writing-review & editing.

#### Declaration of competing interest

The authors declare no conflict of interest.

#### Declaration of Generative AI and AI-assisted technologies in the writing process

The authors confirm that there was no use of artificial intelligence (AI)-assisted technology for assisting in the writing or editing of the manuscript and no images were manipulated using AI.

#### Acknowledgment

The authors thank Jeu-Ming P. Yuann for his assistance with the experimental work.

#### References

- Chopra, I., Roberts, M., 2001. Tetracycline antibiotics: Mode of action, applications, molecular biology, and epidemiology of bacterial resistance. *Microbiology and molecular Biology Reviews: MMBR*, **65**, 232-260. <https://doi.org/10.1128/MMBR.65.2.232-260.2001>
- Roberts, M.C., 1996. Tetracycline resistance determinants: Mechanisms of action, regulation of expression, genetic mobility, and distribution. *FEMS Microbiology Reviews*, **19**, 1-24. <https://doi.org/10.1111/j.1574-6976.1996.tb00251.x>
- Huang ST., Lee SY., Wang SH., Wu CY., Yuann JP., He S., Cheng, C.-W.; Liang, J.-Y., 2019. The influence of the degradation of tetracycline by free radicals from riboflavin-5'-phosphate photolysis on microbial viability. *Microorganisms*, **7**, 500. <https://doi.org/10.3390/microorganisms7110500>
- Alsubih, M., El Morabet, R., Khan, R.A., Khan, N.A., Khan, A.R., Khan, S., Mushtaque, N., Hussain, A., Yousefi, M., 2022. Performance evaluation of constructed wetland for removal of pharmaceutical compounds from hospital wastewater: Seasonal perspective. *Arabian Journal of Chemistry*, **15**, 104344. <https://doi.org/10.1016/j.arabjc.2022.104344>
- Khan, N.A., Vambol, V., Vambol, S., Bolibrukh, B., Sillanpaa, M., Changani, F., Esrafilii, A., Yousefi, M., 2021. Hospital effluent guidelines and legislation scenario around the globe: A critical review. *Journal of Environmental Chemical Engineering*, **9**, 105874. <https://doi.org/10.1016/j.jece.2021.105874>
- Daghrir, R., Drogui, P., 2013. Tetracycline antibiotics in the environment: A review. *Environmental Chemistry Letters*, **11**, 209-227. <https://doi.org/10.1007/s10311-013-0404-8>
- Del Rosso, J.Q., 2015. Oral doxycycline in the management of acne vulgaris: current perspectives on clinical use and recent findings with a new double-scored small tablet formulation. *The Journal of Clinical and Aesthetic Dermatology*, **8**, 19-26.
- Davies, A.K., McKellar, J.F., Phillips, G.O., Reid, A.G., 1979. Photochemical oxidation of tetracycline in aqueous solution. *Journal of the Chemical Society, Perkin Transactions*, **2**, 369-75. <https://doi.org/10.1039/P29790000369>
- Yuann, J.P., Lee, S.Y., He, S., Wong, T.W., Yang, M.J., Cheng, C.W., Huang, S.T., Liang, J.Y., 2022. Effects of free radicals from doxycycline hyclate and minocycline hydrochloride under blue light irradiation on the deactivation of *Staphylococcus aureus*, including a methicillin-resistant strain. *Journal of Photochemistry and Photobiology. B, Biology*, **226**, 112370. <https://doi.org/10.1016/j.jphotobiol.2021.112370>
- Saghi, M., Mahanpoor, K., 2017. Photocatalytic degradation of tetracycline aqueous solutions by nanospherical  $\alpha$ -Fe<sub>2</sub>O<sub>3</sub> supported on 12-tungstosilicic acid as catalyst: Using full factorial experimental design. *International Journal of Industrial Chemistry*, **8**, 297-313. <https://doi.org/10.1007/s40090-016-0108-6>
- Yamal-Turbay, E., Jaén, E., Graells, M.ès, Pérez-Moya, M., 2013. Enhanced photo-Fenton process for tetracycline degradation using efficient hydrogen peroxide dosage. *Journal of Photochemistry and Photobiology A: Chemistry*, **267**, 11-16. <https://doi.org/10.1016/j.jphotochem.2013.05.008>
- Yousefi, M., Farzadkia, M., Mahvi, A.H., Kermani, M., Gholami, M., Esrafilii, A., 2024. Photocatalytic degradation of ciprofloxacin using a novel carbohydrate-based nanocomposite from aqueous solutions. *Chemosphere*, **349**, 140972. <https://doi.org/10.1016/j.chemosphere.2023.140972>
- Cai, F., Tang, Y., Chen, F., Yan, Y., Shi, W., 2015. Enhanced visible-light-driven photocatalytic degradation of tetracycline by Cr<sup>3+</sup> doping SrTiO<sub>3</sub> cubic nanoparticles. *RSC Advances*, **5**, 21290-6. <https://doi.org/10.1039/C4RA13821J>
- Bouafia-Chergui, S., Zemmouri, H., Chabani, M., Bensmail, A., 2016. TiO<sub>2</sub>-photocatalyzed degradation of tetracycline: kinetic study, adsorption isotherms, mineralization and toxicity reduction. *Desalination and Water Treatment*, **57**, 16670-7. <https://doi.org/10.1080/19443994.2015.1082507>
- Reyes, C., Fernandez, J., Freer, J., Mondaca, M., Zaror, C., Malato, S., Mansilla, H.D., 2006. Degradation and inactivation of tetracycline by TiO<sub>2</sub> photocatalysis. *Journal of Photochemistry and Photobiology A: Chemistry*, **184**, 141-6. <https://doi.org/10.1016/j.jphotochem.2006.04.007>

16. Wang, H., Yao, H., Pei, J., Liu, F., Li, D., 2016. Photodegradation of tetracycline antibiotics in aqueous solution by UV/ZnO. *Desalination and Water Treatment*, 57, 19981-19987. <https://doi.org/10.1080/19443994.2015.1103309>
17. Fallahzadeh, S., Yousefi, M., Ghasemi, A., Sadat, S.A., Mohtashemi, M., Rezagholizade-shirvan, A., Naghmachi, M., 2025. Antibacterial and biofilm inhibition of helicobacter pylori using green synthesized MWCNTs/ZnO/Chitosan anocomposites. *Environmental Technology & Innovation*, 38, 104068. <https://doi.org/10.1016/j.eti.2025.104068>
18. Wu, S.C., Huang, J.-W., Liang, C., 2020. Reductive degradation of 1,1,1-trichloroethane with alkaline green tea/ferrous ion in aqueous phase. *Industrial & Engineering Chemistry Research*, 59, 19093-19101. <https://doi.org/10.1021/acs.iecr.0c03443>
19. Balasundram, N., Sundram, K., Samman, S., 2006. Phenolic compounds in plants and agri-industrial by-products: Antioxidant activity, occurrence, and potential uses. *Food Chemistry*, 99, 191-203. <https://doi.org/10.1016/j.foodchem.2005.07.042>
20. Pan, X., Niu, G., Liu, H., 2003. Microwave-assisted extraction of tea polyphenols and tea caffeine from green tea leaves. *Chemical Engineering and Processing: Process Intensification*, 42, 129-133. [https://doi.org/10.1016/s0255-2701\(02\)00037-5](https://doi.org/10.1016/s0255-2701(02)00037-5)
21. Grzesik, M., Naparko, K., Bartosz, G., Sadowska-Bartosza, I., 2018. Antioxidant properties of catechins: Comparison with other antioxidants. *Food Chemistry*, 241, 480-492. <https://doi.org/10.1016/j.foodchem.2017.08.117>
22. Shi, M., Nie, Y., Zheng, X.Q., Lu, J.L., Liang, Y.R., Ye, J.H., 2016. Ultraviolet B (UVB) photosensitivities of tea catechins and the relevant chemical conversions. *Molecules (Basel, Switzerland)*, 21, 1345. <https://doi.org/10.3390/molecules21101345>
23. Yang, M.J., Hung, Y.A., Wong, T.W., Lee, N.Y., Yuann, J.P., Huang, S.T., Wu, C.Y., Chen, I.Z., Liang, J.Y., 2018. Effects of blue-light-induced free radical formation from catechin hydrate on the inactivation of acinetobacter baumannii, including a carbapenem-resistant Strain. *Molecules (Basel, Switzerland)*, 23, 1631. <https://doi.org/10.3390/molecules23071631>
24. Huang, D., Ou, B., Prior, R.L., 2005. The chemistry behind antioxidant capacity assays. *Journal of Agricultural and Food Chemistry*, 53, 1841-1856. <https://doi.org/10.1021/jf030723c>
25. Dube, A., Ng, K., Nicolazzo, J.A., Larson, I., 2010. Effective use of reducing agents and nanoparticle encapsulation in stabilizing catechins in alkaline solution. *Food Chemistry*, 122, 662-667. <https://doi.org/10.1016/j.foodchem.2010.03.027>
26. Ye, Q., Chen, H., Zhang, L.B., Ye, J.H., Lu, J.L., Liang, Y.R., 2009. Effects of temperature, illumination, and sodium ascorbate on browning of green tea infusion. *Food Science and Biotechnology*, 18, 932-8.
27. Zhu, Q.Y., Zhang, A., Tsang, D., Huang, Y., Chen, Z.-Y., 1997. Stability of green tea catechins. *Journal of Agricultural and Food Chemistry*, 45, 4624-4628. <https://doi.org/10.1021/jf9706080>
28. Janeiro, P., Oliveira Brett, A.M., 2004. Catechin electrochemical oxidation mechanisms. *Analytica Chimica Acta*, 518, 109-115. <https://doi.org/10.1016/j.aca.2004.05.038>
29. Mochizuki, M., Yamazaki, S., Kano, K., Ikeda, T., 2002. Kinetic analysis and mechanistic aspects of autooxidation of catechins. *Biochimica et Biophysica Acta*, 1569, 35-44. [https://doi.org/10.1016/s0304-4165\(01\)00230-6](https://doi.org/10.1016/s0304-4165(01)00230-6)
30. Chen, L.-Y., Wu, J.-Y., Liang, J.-yuan, 2018. Using chromatography and mass spectrometry to monitor isomerization of catechin in alkaline aqueous with thermal processing. *Journal of Food Processing and Preservation*, 42, e13365. <https://doi.org/10.1111/jfpp.13365>
31. Chen, L.Y., Cheng, C.W., Liang, J.Y., 2015. Effect of esterification condensation on the Folin-Ciocalteu method for the quantitative measurement of total phenols. *Food Chemistry*, 170, 10-15. <https://doi.org/10.1016/j.foodchem.2014.08.038>
32. Huang, S.T., Hung, Y.A., Yang, M.J., Chen, I.Z., Yuann, J.P., Liang, J.Y., 2019. Effects of epigallocatechin gallate on the stability of epicatechin in a photolytic process. *Molecules (Basel, Switzerland)*, 24, 787. <https://doi.org/10.3390/molecules24040787>
33. Nkere, C.K., Ibe, N.I., Iroegbu, C.U., 2011. Bacteriological quality of foods and water sold by vendors and in restaurants in Nsukka, Enugu State, Nigeria: A comparative study of three microbiological methods. *Journal of Health, Population, and Nutrition*, 29, 560-566. <https://doi.org/10.3329/jhpn.v29i6.9892>
34. Kozuskanich, J., Novakowski, K.S., Anderson, B.C., 2011. Fecal indicator bacteria variability in samples pumped from monitoring wells. *Ground Water*, 49, 43-52. <https://doi.org/10.1111/j.1745-6584.2010.00713.x>
35. Clementi, C., Cesaretti, A., Carlotti, B., Elisei, F., 2016. The Role of pH in modulating the electronic state properties of minocycline drug and its inclusion within micellar carriers. *The Journal of Physical Chemistry. A*, 120, 4994-5005. <https://doi.org/10.1021/acs.jpca.5b12707>
36. Yuann, J.-M.P., Lee, S.-Y., Yang, M.-J., Huang, S.-T., Cheng, C.-W., Liang, J.-Y., 2021. A study of catechin photostability using photolytic processing. *Processes*, 9, 293. <https://doi.org/10.3390/pr9020293>
37. Peng, H., Shahidi, F., 2023. Oxidation and degradation of (epi)gallocatechin gallate (EGCG/GCG) and (epi)catechin gallate (ECG/CG) in alkali solution. *Food Chemistry*, 408, 134815. <https://doi.org/10.1016/j.foodchem.2022.134815>
38. Liang, J.Y., Wu, J.Y., Yang, M.Y., Hu, A., Chen, L.Y., 2016. Photo-catalytic polymerization of catechin molecules in alkaline aqueous. *Journal of Photochemistry and Photobiology. B, Biology*, 165, 115-120. <https://doi.org/10.1016/j.jphotobiol.2016.10.020>
39. Dueñas, M., González-Manzano, S., González-Paramás, A., Santos-Buelga, C., 2010. Antioxidant evaluation of O-methylated metabolites of catechin, epicatechin and quercetin. *Journal of Pharmaceutical and Biomedical Analysis*, 51, 443-449. <https://doi.org/10.1016/j.jpba.2009.04.007>
40. Neta, P., Huie, R.E., Maruthamuthu, P., Steenken, S., 1989. Solvent effects in the reactions of peroxy radicals with organic reductants: Evidence for proton-transfer-mediated electron transfer. *The Journal of Physical Chemistry*, 93, 7654-7659. <https://doi.org/10.1021/j100359a025>
41. Nakayama, T., Ichiba, M., Kuwabara, M., Kajiya, K., Kumazawa, S., 2002. Mechanisms and structural specificity of hydrogen peroxide formation during oxidation of Catechins. *Food Science and Technology Research*, 8, 261-267. <https://doi.org/10.3136/fstr.8.261>
42. Roginsky, V., Alegria, A.E., 2005. Oxidation of tea extracts and tea catechins by molecular oxygen. *Journal of Agricultural and Food Chemistry*, 53, 4529-4535. <https://doi.org/10.1021/jf040382i>
43. Jovanovic, S.V., Steenken, S., Tosic, M., Marjanovic, B., Simic, M.G., 1994. Flavonoids as antioxidants. *Journal of the American Chemical Society*, 116, 4846-4851. <https://doi.org/10.1021/ja00090a032>
44. Volkens, G., Damas, J.M., Palm, G.J., Panjikar, S., Soares, C.M., Hinrichs, W., 2013. Putative dioxygen-binding sites and recognition of tigeicycline and minocycline in the tetracycline-degrading monooxygenase TetX. *Acta crystallographica. Section D, Biological Crystallography*, 69, 1758-1767. <https://doi.org/10.1107/S0907444913013802>
45. Zhong, S.F., Yang, B., Xiong, Q., Cai, W.W., Lan, Z.G., Ying, G.G., 2022. Hydrolytic transformation mechanism of tetracycline antibiotics: Reaction kinetics, products identification and determination in WWTPs. *Ecotoxicology and Environmental Safety*, 229, 113063. <https://doi.org/10.1016/j.ecoenv.2021.113063>
46. Verloop, A.J.W., Vincken, J.-P., Gruppen, H., 2016. Peroxidase can perform the hydroxylation step in the "oxidative cascade" during oxidation of tea catechins. *Journal of Agricultural and Food Chemistry*, 64, 8002-8009. <https://doi.org/10.1021/acs.jafc.6b03029>
47. Yang, W., Moore, I.F., Koteva, K.P., Bareich, D.C., Hughes, D.W., Wright, G.D., 2004. TetX is a flavin-dependent monooxygenase conferring resistance to tetracycline antibiotics. *The Journal of Biological Chemistry*, 279, 52346-52352. <https://doi.org/10.1074/jbc.M409573200>
48. Martinez, S., Valek, L., Petrović, Ž., Metikoš-Huković, M., Piljac, J., 2005. Catechin antioxidant action at various pH studied by cyclic voltammetry and PM3 semi-empirical calculations. *Journal of Electroanalytical Chemistry*, 584, 92-99. <https://doi.org/10.1016/j.jelechem.2005.07.015>
49. Gu, L., Kelm, M.A., Hammerstone, J.F., Zhang, Z., Beecher, G., Holden, J., Haytowitz, D., Prior, R.L., 2003. Liquid chromatographic/electrospray ionization mass spectrometric studies of proanthocyanidins in foods. *Journal of Mass Spectrometry: JMS*, 38, 1272-1280. <https://doi.org/10.1002/jms.541>
50. Li, H.J., Deinzer, M.L., 2007. Tandem mass spectrometry for sequencing proanthocyanidins. *Analytical Chemistry*, 79, 1739-1748. <https://doi.org/10.1021/ac061823v>
51. Drynan, J.W., Clifford, M.N., Obuchowicz, J., Kuhnert, N., 2010. The chemistry of low molecular weight black tea polyphenols. *Natural Product Reports*, 27, 417-462. <https://doi.org/10.1039/b912523j>
52. He, F., Pan, Q.H., Shi, Y., Duan, C.Q., 2008. Biosynthesis and genetic regulation of proanthocyanidins in plants. *Molecules (Basel, Switzerland)*, 13, 2674-2703. <https://doi.org/10.3390/molecules13102674>
53. Yang, M.-J., Lee, S.-Y., Chen, S.-H., Huang, S.-T., Cheng, C.-W., Chiu, C.-M., Yuann, J.-M.P., Liang, J.-Y., 2023. The effect of sodium citrate on the photolytic reaction of catechin following the addition of aluminum chloride under alkaline conditions. *Journal of Photochemistry and Photobiology A: Chemistry*, 445, 115051. <https://doi.org/10.1016/j.jphotochem.2023.115051>
54. Crozier, A., Jaganath, I.B., Clifford, M.N., 2009. Dietary phenolics: Chemistry, bioavailability and effects on health. *Natural Product Reports*, 26, 1001-1043. <https://doi.org/10.1039/b802662a>
55. Legeay, S., Rodier, M., Fillon, L., Faure, S., Clere, N., 2015. Epigallocatechin gallate: A Review of its beneficial properties to prevent metabolic syndrome. *Nutrients*, 7, 5443-5468. <https://doi.org/10.3390/nu7075230>
56. Hammerstone, J.F., Lazarus, S.A., Schmitz, H.H., 2000. Procyanidin content and variation in some commonly consumed foods. *The Journal of Nutrition*, 130, 2086S-2092S. <https://doi.org/10.1093/jn/130.8.2086S>
57. Prior, R.L., Lazarus, S.A., Cao, G., Muccitelli, H., Hammerstone, J.F., 2001. Identification of procyanidins and anthocyanins in blueberries and cranberries (*Vaccinium* spp.) using high-performance liquid chromatography/mass spectrometry. *Journal of Agricultural and Food Chemistry*, 49, 1270-1276. <https://doi.org/10.1021/jf001211q>
58. Wollgast, J., Pallaroni, L., Agazzi, M.E., Anklam, E., 2001. Analysis of procyanidins in chocolate by reversed-phase high-performance liquid chromatography with electrospray ionisation mass spectrometric and tandem mass spectrometric detection. *Journal of Chromatography. A*, 926, 211-220. [https://doi.org/10.1016/s0021-9673\(01\)00994-3](https://doi.org/10.1016/s0021-9673(01)00994-3)
59. Cos, P., De Bruyne, T., Hermans, N., Apers, S., Berghe, D.V., Vlietinck, A.J., 2004. Proanthocyanidins in health care: Current and new trends. *Current Medicinal Chemistry*, 11, 1345-1359. <https://doi.org/10.2174/0929867043365288>